2

The shapes of planets and moons

> The equal gravitation of the parts on all sides would give a spherical figure to the planets, if it was not for their diurnal revolution in a circle ….
> I. Newton, *Principia*, Theorem XVI

Modern space exploration has made everyone familiar with the idea that planets are mostly spherical. From a great distance a casual observer might not even notice that rotating planets and moons are not quite perfect spheres. However, careful examination reveals departures from perfection. Rotating planets are slightly oblate spheres, while tidally locked satellites are triaxial. Furthermore, once these bodies are approached closely, it becomes clear that nearly every planet and moon possesses topographic variations. Mountains, valleys, plains, and craters create landscapes that, up close, can challenge attempts to traverse them by mechanical rovers or human explorers.

The forces that create and maintain the topography of planetary bodies depend on the scale of the feature. The gravitational self-attraction that tends to make planets spherical operates differently on the scale of individual mountains. It is thus useful to distinguish several *orders of relief* that categorize different scales of topographic feature. This notion can be made mathematically precise through the use of spherical harmonics, a concept that will be discussed later in this chapter.

The tendency of large masses of material to take on a spherical shape was first recognized by Isaac Newton (1643–1727) in 1686. His brilliant insight into universal gravitation showed that, in the absence of other forces, the attraction of matter for other matter tends to mould all bodies into spheres. Gravity is weak compared to other forces so, on a human scale, bodies must be very large for gravity to dominate the electromagnetic forces that give atomic matter its strength to resist deformation. The conflict between strength and gravitation is the subject of Chapter 3. This chapter concentrates on the largest-scale features of planetary topography and its geometric properties.

Table 2.1 *Physical characteristics of large bodies in the Solar System*

Name	Equatorial radius (km)	Mass (kg)	Mean density (kg/m^3)	Equatorial acceleration of gravity (m/s^2)	Sidereal rotation period
Mercury	2 439	3.303×10^{23}	5430	2.78	58.75 days
Venus	6 051	4.870×10^{24}	5250	8.60	243.01 days
Earth	6 378	5.976×10^{24}	5520	9.78	1.00 days
Moon	1 738	7.349×10^{22}	3340	1.62	27.322 days
Mars	3 393	6.421×10^{23}	3950	3.72	1.029 days
Ceres	424	8.6×10^{20}	1980	0.32	9.08 hours
Vesta	234	3.0×10^{20}	3900	0.37	5.34 hours
Jupiter	71 492[a]	1.900×10^{27}	1330	22.88	9.925 hours[b]
Io	1 815	8.94×10^{22}	3570	1.81	1.769 days
Europa	1 569	4.80×10^{22}	2970	1.30	3.551 days
Ganymede	2 631	1.48×10^{23}	1940	1.43	7.155 days
Callisto	2 400	1.08×10^{23}	1860	1.25	16.689 days
Saturn	60 268[a]	5.688×10^{26}	690	9.05	10.675 hours[b]
Titan	2 575	1.35×10^{23}	1880	1.36	15.945 days
Uranus	25 559[a]	8.684×10^{25}	1290	7.77	17.240 hours[b]
Neptune	24 764[a]	1.02×10^{26}	1640	11.0	16.11 hours[b]
Triton	1 350	2.14×10^{22}	2070	0.78	5.877 days
Pluto	1 150	1.29×10^{22}	2030	0.658	6.3872 days
Charon	604	1.52×10^{21}	1650	0.278	6.3872 days

[a] Measured at the 1-bar pressure level.

[b] Internal rotation period derived from the magnetic field.

2.1 The overall shapes of planets

2.1.1 Non-rotating planets: spheres

The lowest order of relief, which in this book we call the "zeroth order" because it corresponds to the zeroth-order spherical harmonic, is the overall diameter of the body. The shape of a non-rotating, self-gravitating mass of material that has no intrinsic strength is a perfect sphere. We can describe such an object by its radius or diameter, and with this single datum our description of its shape is complete. Of course, the smaller bodies in the Solar System, such as asteroids or small satellites, may depart considerably from a perfect spherical shape, but it is still useful to describe them by the radius of a sphere of equal volume. Most tabulations of the physical properties of the planets and moons give their diameter, along with their mass (see Table 2.1). From the mass and diameter other physically interesting parameters, such as density or the surface acceleration of gravity, can be computed.

The volume V of a sphere of radius r is, as everyone learns in high school, $V = \frac{4}{3}\pi r^3$. Fewer readers may remember that the volume of a triaxial ellipsoid with semiaxes a, b and c is given by the similar formula $V = \frac{4}{3}\pi abc$. Thus, the mean radius (that is, the radius of a sphere of equal volume) of a triaxial body is given by $r_{\text{mean}} = \sqrt[3]{abc}$. In many cases a, b, and c differ only slightly from the mean. When this happens we can use the approximate formula $r_{\text{mean}} \approx (a + b + c)/3$. These simple formulas will prove useful in interpreting the relationships between various radii commonly encountered in tabulations.

2.1.2 Rotating planets: oblate spheroids

Newton himself recognized the first level of deviation from a perfectly spherical shape. Rotating bodies are not spherical: They are oblate spheres with larger equatorial radii than polar radii. In the language of spherical harmonics this is the second order of relief. Historically, the Earth's oblateness was not at all obvious to Newton's contemporaries and sparked a debate between Newton and contemporary astronomer Jacques Cassini (1677–1756) that resulted in one of the first major scientific expeditions, a project to precisely measure and compare the length of a degree of latitude in both France and Lapland. The result, announced in 1738, was the first direct evidence that the Earth is shaped like an oblate spheroid, whose equatorial radius is about 22 km longer than its radius along its axis of rotation. This apparently tiny deviation, of only 22 km out of 6371 km, is expressed by the *flattening* of the Earth, f, defined as:

$$f = \frac{a - c}{a} \tag{2.1}$$

where a is the equatorial radius of the Earth and c is its polar radius (Figure 2.1). The currently accepted value for the Earth's flattening, 1/298.257, is substantially different from Newton's own theoretical estimate of 1/230.

Newton derived his estimate of Earth's oblateness from a theory that assumed that the Earth's density is uniform. Under this assumption he was able to show that the flattening is proportional to a factor m, the ratio between the centrifugal acceleration at the equator (a consequence of rotation) and the gravitational acceleration at the equator. This ratio expresses the tendency of a planet to remain spherical: Smaller m implies that rotation is less important and the planet is more spherical.

$$m = \frac{\omega^2 a^3}{GM} \cong \frac{3}{4\pi}\frac{\omega^2}{G\bar{\rho}}. \tag{2.2}$$

In this equation ω is the rotation rate of the Earth (in radians per second), G is Newton's gravitational constant, 6.672 x 10^{-11} $m^3/kg\text{-}s^2$, M is the mass of the Earth and $\bar{\rho}$ is its mean density. Even in Newton's time it was known that $m \approx 1/290$. Newton used a clever argument involving hypothetical water-filled wells drilled from both the pole and equator that join at the center of the Earth. Supposing that the wellheads are connected by a level canal

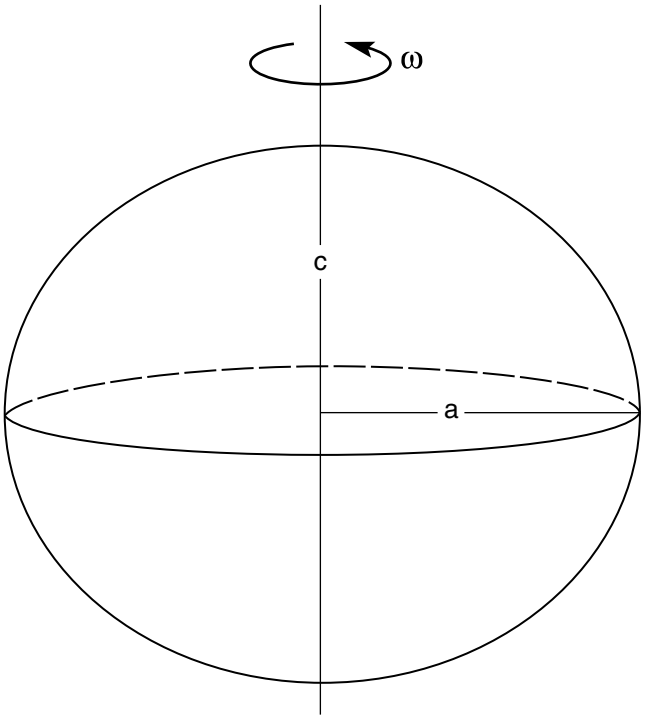

Figure 2.1 Oblate spherical shape of a rotating fluid planet with no strength. The equatorial radius is a, the polar radius is c, and the rotation rate is ω.

at the surface, he used the impossibility of perpetual motion to argue that the pressure at the bottom of the water columns had to be equal at the Earth's center, from which he derived the expression:

$$f = \frac{5}{4}m. \tag{2.3}$$

Although not quite correct for the Earth, this formula gives an excellent first approximation to the flattening.

Implicit in Newton's derivation is the idea that water tends to assume a *level surface*. That is, the surface that water naturally attains coincides with a surface on which the gravitational potential energy is constant. If the surface of a body of water, or any other strengthless fluid, did not follow a constant gravitational potential, it could gain energy by flowing downhill. Thus, in the absence of currents or other imposed pressure gradients, the surface of a fluid must coincide with an *equipotential*. This is sometimes called an *equilibrium surface*. This proposition holds equally well for planetary atmospheres, which also tend to have equal pressures on equipotential surfaces. It is important to note that on a rotating planet the equilibrium surface is not a sphere but an oblate spheroid (on very rapidly

rotating bodies this surface becomes still more complex, but such surfaces do not seem to be important on any currently known planets). In real planets, lateral variations in density lead to further distortions of the equilibrium surfaces. An arbitrarily chosen equilibrium surface, called the *geoid*, forms the primary reference from which topographic elevations are measured on Earth. Deviations of a planet's surface from an equilibrium surface must be supported by strength.

Several hundred years of further effort by mathematical physicists were needed to extend Newton's simple flattening estimate to a more comprehensive form. In 1959 Sir Harold Jeffreys established a formula for the flattening of a rotating, strengthless body in hydrostatic equilibrium (for which contours of constant density coincide with equipotentials at all depths within the body). This more complicated formula is:

$$f = \frac{\frac{5}{2}m}{1+\frac{25}{4}\left[1-\frac{3}{2}\left(\frac{C}{Ma^2}\right)\right]^2} \tag{2.4}$$

where C is the planet's moment of inertia about the polar axis. The moment of inertia is defined as the integral:

$$C = \int_o^M r^2 dm \tag{2.5}$$

where r is the radial distance of the infinitesimal mass element dm from the axis about which C is computed. In the case of the polar moment of inertia C this is the rotation axis.

The dimensionless moment of inertia ratio, C/Ma^2, expresses the concentration of mass toward the center of the planet. This ratio is equal to zero for a point mass, equals 2/5 (= 0.4) for a uniform density sphere and is measured to be 0.33078 for the Earth. Earth's moment of inertia ratio is less than 0.4 because mass is concentrated in its dense nickel–iron core. In the uniform density case, $C/Ma^2 = 2/5$, and Equation (2.4) reduces exactly to Newton's estimate.

Newton's contemporaries also noted the rather large flattening of the rapidly rotating planets Jupiter and Saturn. Modern measurements of the flattening of the planets in our Solar System are listed in Table 2.2.

Mars is a special case. Its observed shape flattening, $f_{\text{Mars}} = 1/154$ is considerably larger than that estimated from Jeffreys' formula above, which gives $f = 1/198$. This is because Mars is far from hydrostatic equilibrium, and so violates the assumptions of Jeffreys' derivation. The Tharsis Rise volcanic complex is so large and so massive that it dominates the gravitational field of the planet and warps its shape well out of hydrostatic equilibrium. Its equatorial radius varies by almost 5 km, depending on longitude. Geophysical models of Mars have yet to fully separate the effects of Tharsis from the radial concentration of mass towards its core. The shapes of small bodies in the Solar System – comets, asteroids and

Table 2.2 *Deviations of Solar System bodies from spheres*

Name	Moment of inertia factor, C/MR^2	Topographic flattening	Dynamical flattening	Center of mass – center of figure offset (km)
Mercury	0.33	~1/1800.	1/1.03 x 10^6	?
Venus	0.33	0	1/1.66 x 10^7	0.280
Earth	0.33078	1/298.257	1/301	2.100
Moon	0.394	1/801.6	1/1.08 x 10^5	1.982
Mars	0.366	1/154.	1/198.	2.501
Jupiter	0.254	1/15.42[a]	1/15.2	–
Saturn	0.210	1/10.2[a]	1/10.2	–
Uranus	0.225	1/43.6[a]	1/50.7	–
Neptune	0.24	1/58.5[a]	1/54.4	–

Data from Yoder (1995).

[a] At 1-bar pressure level in the atmosphere.

small moons – do not obey Jeffreys' formula for similar reasons; their inherent strength produces large departures from hydrostatic equilibrium.

Mercury is another interesting planet from the flattening perspective. Although we do not know its flattening very accurately (not to better than 10%), it seems to be very small, about 1/1800. This is consistent with its current slow rotation period of about 57 days. However, Mercury is so close to the Sun that it is strongly affected by solar tides. It may originally have had a much faster rotation rate that has since declined, placing the planet in its current 3/2 spin-orbital resonance with the Sun (that is, Mercury rotates three times around its axis for every two 88-day trips around the Sun). If this is correct, then Mercury's flattening may have changed substantially over the history of the Solar System. Chapter 4 will discuss the tectonic consequences of this global shape change.

2.1.3 Tidally deformed bodies: triaxial ellipsoids

After rotation, the next degree of complication in planetary shapes includes the effects of tidal forces. Tides are the result of the variation of the gravitational potential of a primary attractor across the body of an orbiting satellite, along with the centripetal potential due to its orbit about the primary. The consequence of these varying potentials on a mostly spherical satellite is that it becomes elongated along the line connecting the centers of the primary and satellite, compressed along its polar axis, and compressed by an intermediate amount along the axis tangent to its orbit (Figure 2.2).

If the satellite (and this includes the planets themselves, which are satellites of the Sun) spins at a rate different than its orbital period, then the elongation of the equipotential surface in a frame of reference rotating with the satellite varies with time. A point on the

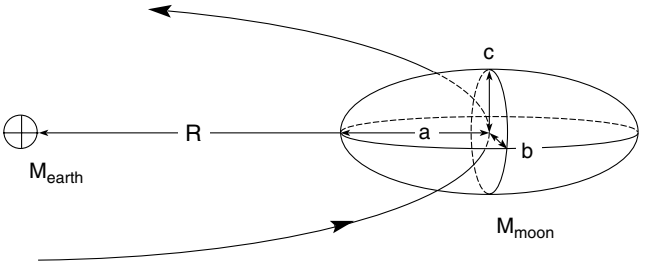

Figure 2.2 Tidal deformation of a synchronously rotating satellite such as our Moon, orbiting about its primary at a distance R. The tidal forces stretch the satellite along the line connecting its center to that of its primary such that the radius a along this line is larger than any of its other principal radii. The smallest radius c is perpendicular to the orbital plane and the intermediate radius b is parallel to the orbit's tangent.

equator is alternately lifted and dropped as it rotates from the line between its center and that of the primary, to the line tangent to the orbit. These periodic equipotential changes, which on Earth we recognize as the force responsible for oceanic tides, create motions that dissipate rotational energy and, for strong enough tides or long enough times, may eventually slow the satellite's rotation. The Earth is subject to both solar and lunar tides, which have gradually lengthened our day from 18 hours, 1.3 billion years ago, to its present 24 hours. The Moon, being less massive than the Earth, long ago lost any excess rotation and is now synchronously locked to the Earth, rotating once on its axis for each orbit around the Earth. Many other satellites in the Solar System are similarly synchronously locked to their primaries, including the four large Galilean satellites of Jupiter and Saturn's large satellite Titan. Mercury itself is an exception. Although astronomers long believed that Mercury is synchronously locked to the Sun, we now understand that its highly elliptical orbit led it to be trapped in the present 3/2 spin-orbit resonance.

Tidal forces produce a characteristic pattern of deformation on synchronously rotating satellites. Harold Jeffreys, in his famous book *The Earth* (Jeffreys, 1952), showed that the equipotential surface of a tidally locked body is a triaxial ellipsoid with three unequal axes $a>b>c$. The lengths of these axes are:

$$a = r_{\text{moon}}\left(1+\frac{35}{12}\Omega\right)$$

$$b = r_{\text{moon}}\left(1-\frac{10}{12}\Omega\right)$$

$$c = r_{\text{moon}}\left(1-\frac{25}{12}\Omega\right) \tag{2.6}$$

where r_{moon} is the mean radius of the Moon. It is clear that the average of these three axial distances just equals the mean radius. These distortions depend on the dimensionless factor Ω, given by:

$$\Omega = \frac{M_{earth}}{M_{moon}} \frac{r_{moon}^3}{R^3} \tag{2.7}$$

where M_{earth} and M_{moon} are the masses of the Earth and Moon, respectively, and R is the distance between the Earth and the Moon.

Naturally, for satellites other than the Moon orbiting about some other primary, the analogous quantities must be inserted in Ω. The distortion is larger for a larger ratio between primary mass and satellite mass and smaller for increased distance between the two bodies. Jeffreys' equations above are strictly valid only for a Moon of uniform density. The book by Murray and Dermott (1999) describes how to treat the general case where the Moon's density is not uniform. Table 2.3 lists the ratios between the different axes of the satellites in the Solar System for which they are known.

According to the formulas (2.6) and (2.7), the maximum difference between the axes, $a - c$, on Earth's Moon is presently about 66 m. The Moon is 10 to 20 times more distorted than this, a fact that was known even in Harold Jeffreys' day. The current best estimates indicate that the Moon is at least 10 times more distorted than the hydrostatic prediction. This observation prompted Jeffreys to propose that the present figure of the Moon is the fossil remnant of a formerly much larger distortion. The Moon is presently receding from the Earth at the rate of about 3.8 cm/year. This recession rate was surely higher in the past when the Moon was closer to the Earth and tides were, therefore, higher (the full story of the evolution of the Moon's orbit is a complicated one, involving changes in tidal dissipation over the age of the Earth as continents and seas shifted). Nevertheless, it is clear that the Moon was once much closer to the Earth than it is now. Because the lengths of the axes depend on the Earth–Moon distance to the inverse cube power, Jeffreys postulated that the present figure could have been frozen-in at a time when the Moon was about 1/2.7 times its present distance from the Earth. At this distance the Moon would have circled the Earth in only 6.1 days and, by angular momentum conservation, a day on Earth would have lasted only 8.2 hours.

The major problem with Jeffreys' proposal (which he recognized himself) is that the hydrostatic formulas (2.6) make a definite prediction that that the ratio $(a - c)/(b - c) = 4$, independent of the Earth–Moon distance. The latest value of this ratio from Japan's Kaguya mission (Araki *et al.*, 2009) is 1.21, far from the hydrostatic value of 4. The general opinion at the present time is that, although the Moon clearly departs from a hydrostatic shape, the present shape is more a consequence of geologic forces that sculpted the lunar surface rather than the remnant of a former hydrostatic figure.

In examining Table 2.3 the ratio of axes differences in the last column is more often quite different from the theoretical value of 4 than close to it. The larger satellites approach most closely to this ideal ratio, while the smaller ones are clearly dominated by strength rather than gravitational forces.

Table 2.3 *Triaxial shapes of small satellites*

Name	Density (kg/m^3)	Mean radius (km)	(a–c) (km)	(a–c)/ (b–c)
Earth's Satellite				
Moon[a]	3340	1737	0.713	1.21
Martian Satellites				
Phobos[b]	1900	11.1	4.0	2.2
Deimos[b]	1760	6.3	2.1	2.6
Jovian Satellites				
Metis[c]	3000	21.7	13.0	4.3
Adrastea[c]	3000	8.2	3.0	3.0
Almathea[c]	862	83.6	61.0	6.8
Thebe[c]	3000	49.2	16.0	2.3
Io[d]	3528	1818.1	14.3	4.1
Europa[d]	3014	1560.7	3.0	3.8
Ganymede[d]	1942	2634.1	1.8	4.5
Callisto[d]	1834	2408.3	0.2	2.0
Saturnian Satellites				
Mimas[e]	1150	198.1	16.8	2.7
Enceladus[e]	1608	252.1	8.3	2.7
Tethys[e]	973	533.0	12.9	3.6
Dione[e]	1476	561.7	3.5	5.0
Rhea[e]	1233	764.3	4.1	−6.8
Titan[f]	1881	2574.5	0.410	3.8
Iapetus[e]	1083	723.9	35.0	n/a
Uranian Satellites				
Miranda[g]	1200	235.7	7.1	5.5
Ariel[g]	1670	578.9	3.4	17.0

Data from:
[a] Araki *et al.* (2009)
[b] Thomas (1989)
[c] Thomas *et al.* (1998)
[d] Davies *et al.* (1998)
[e] Thomas *et al.* (2007)
[f] Iess *et al.* (2010)
[g] Thomas (1988)

Most of the other moons in the Solar System depart substantially from a hydrostatic shape. However, it appears that the shape of Jupiter's large, tidally heated moons Io and Europa may be close to equilibrium ellipsoids. If that is the case, then the maximum distortion, a–c, should be 14.3 km for Io and 3.9 km for Europa. The Galileo spacecraft

confirmed these expectations with an accuracy of 0.12 and 0.65 km, respectively (Davies *et al.*, 1998).

2.1.4 A scaling law for planetary figures?

William Kaula (1926–2000), who contributed extensively to understanding the figure of the Earth from satellite measurements, proposed a scaling law that seems to approximately give the deviations of planetary figures from a hydrostatic shape. The law is based on the idea that all planets have about the same intrinsic strength, and that stress differences are proportional to the surface acceleration of gravity, g (Kaula, 1968, p. 418). In the absence of any other information about a planet, this law may give a useful first estimate of how far a "normal" planet's figure departs from the hydrostatic shape.

This departure is given by Kaula's first law:

$$\left.\frac{C-A}{Ma^2}\right|_{\text{non-hydrostatic}} \propto \frac{1}{g^2} \tag{2.8}$$

where C and A are the moments of inertia about the shortest and longest axes of the figure, respectively. The difference in moments of inertia is proportional to the normalized difference of the lengths of the axes, $(a\text{-}c)/a$, so that this rule also implies that the deviations of this ratio from its hydrostatic value should depend on the inverse square of the gravitational acceleration. For constant density, g is proportional to the planetary radius, so this ratio should equally depend on the inverse square of the planetary radius. Looking ahead to Chapter 3, we will see in Section 3.3.3 and Figure 3.5 that this relation does seem to hold approximately in our Solar System for the larger bodies, but it fails badly for small objects for which strength is controlled by frictional forces that depend on pressure.

The possibility that planets may have substantial non-hydrostatic contributions to their figures plays an important role in studies of rotational dynamics and the tidal evolution of bodies in the Solar System. For example, the present orientation of the Moon with respect to the Earth may be partly due to the distribution of dense lavas in the low-lying basins on the nearside. The orientation of Mercury may be controlled by mass anomalies associated with the Caloris Basin. And if Europa has too large a non-hydrostatic figure, then its putative slow non-synchronous rotation cannot occur.

2.1.5 Center of mass to center of figure offsets

One of the widely publicized results of the Apollo missions to the Moon was the discovery that the Moon's center of mass is about 2 km closer to the Earth than its center of figure. For many years this offset was known only in the Moon's equatorial plane, as all of the Apollo flights circled the Moon's equator. Now, as a result of the unmanned Clementine mission, we know more precisely that the offset is 1.982 km.

Although, in hindsight, it is not really surprising that such an offset should exist, the possibility that the center of figure of a planet might not correspond with its center of mass was never considered in classical geodesy. All harmonic expansions of the gravity field of the Earth are made about its center of mass and so the reference geoid and all other equipotential surfaces are also centered about this point. In fact, the Earth itself has a substantial center of mass – center of figure offset if the water filling the ocean basins is neglected. The floor of the Pacific Ocean is about 5 km below sea level, whereas the opposite hemisphere is dominated by the continental landmasses of Asia, Africa, and the Americas. The waterless Earth's center of figure is thus offset from its center of mass by about 2.5 km at the present time. Of course, as the continents drift around over geologic time this offset gradually changes in both direction and magnitude. The fundamental reason for the offset is the difference in density and thickness between oceanic crust and continental crust. Table 2.2 lists these offsets for the bodies where they are known.

For reasons that are still not understood, most of the terrestrial planets show striking asymmetries on a hemispheric scale. The nearside of the Moon looks quite different from the farside, and lies at a lower average elevation with respect to its center of mass. It is generally believed that this is due to a thicker crust on the farside, although what caused the thickness variation is unknown. Mars also possesses a strong hemispheric asymmetry. The northern plains of Mars lie an average of 5 km lower than the southern highlands. Here again the immediate cause may be a difference in crustal thickness or composition, but the ultimate reason for the difference is presently unknown.

2.1.6 Tumbling moons and planets

Most rotating bodies in the Solar System spin about an axis that coincides with their maximum moment of inertia, the C axis in our terminology. The moment of inertia is actually a second-rank tensor, written I_{ij}, which can be defined for any solid body as a generalization of the definition (2.5) for C:

$$I_{ij} = \int r_i r_j \, \mathrm{d}m \tag{2.9}$$

where the subscripts i and j run from 1 to 3 and denote, respectively, the x, y, and z axes of a Cartesian coordinate system. The symbol r_i for $i = 1$, 2, and 3, thus, denotes the x, y, and z coordinates of a mass element dm with respect to the origin around which the moment of inertia is computed, generally taken to be the center of mass of a body.

A fundamental theorem of tensor mathematics states that a suitable rotation of the coordinate axes can always be found in which the tensor (2.9) is diagonal (that is $I_{ij} = 0$ unless $i = j$) about three perpendicular axes. The moments of inertia about these special axes are called the principal moments of inertia and are labeled C, B, and A for the maximum, intermediate, and minimum principal moments, $C \geq B \geq A$. The lengths of the corresponding principal axes are conventionally written in lower case and, perhaps confusingly, the c axis is usually the *shortest* of the three: $c \leq b \leq a$. The reason for this inverse order is that the

moment of inertia is largest about that axis for which the mass elements are most distant and, thus, the r_i perpendicular to the axis are largest.

The reason that the C axis is special is that a body that rotates about this axis has the lowest kinetic energy possible for a fixed angular momentum. Angular momentum is conserved for an isolated body, but kinetic energy can be converted into heat. A body rotating about the A axis, say, spins relatively quickly but this is the highest-energy rotational state, so if it exchanges kinetic energy for heat it must spin about another axis, or a combination of axes in a complex tumbling motion. When the body finally spins about its C axis it attains a minimum energy configuration and cannot change its rotation further (unless some external torque acts on it).

This lesson was learned the hard way in the early days of space exploration when the first US satellite, Explorer 1, which was shaped like a long narrow cylinder, was stabilized by spinning it around its long axis. A broken antenna connection flexed back and forth as the satellite rotated, dissipating energy. Within hours the satellite was spinning about its C axis – the short axis, perpendicular to the cylinder. Because the spacecraft was not designed to operate in this configuration radio contact was soon lost.

Most Solar System bodies, therefore, spin about their C axes. A few small asteroids have been discovered that are in "excited" rotation states in which the object is not in its minimum-energy rotational state and thus tumbles, but these exceptions are rare because nearly every object has some means of dissipating energy internally and thus eventually seeks out the lowest energy configuration.

Mars is a prime example of the importance of this process. Mars' major positive gravity anomaly, the Tharsis Rise, is located on its equator. This location puts the excess mass as far as possible from its rotational axis, maximizing the moment of inertia. The opposite extreme is illustrated by the asteroid Vesta, which suffered an impact that gouged out a crater (a mass deficit) nearly as large in diameter as Vesta itself. The central peak of this crater is now located at its rotational pole (which happens to be the south pole), the most stable configuration.

2.2 Higher-order topography: continents and mountains

2.2.1 How high is high?

As silly as this question may seem, it highlights a common assumption that underlies our thinking when we consider the elevation of some topographic feature. An elevation is a number or contour that we read off a map (or, more commonly in modern times, a color code on an image). But what is that elevation *relative* to? Does it directly give the distance from the center of the planet? Or the height above an arbitrary spheroid? Or, more commonly on Earth, the elevation above mean sea level? The answer to all these questions is, "it depends."

The fundamental reference surface for elevations, or *geodetic datum*, is established empirically. Historically, it has varied with the technology for measuring topography,

completeness or accuracy of information and, sometimes, pure convenience. The era of space exploration has brought great changes in this type of measurement, as well as bringing new planets under close scrutiny. Each new planet has presented unique challenges in the apparently simple task of measuring the elevations of its surface features.

In the case of the Earth, detailed mapping began in the eighteenth century with trigonometric surveys utilizing telescopes, carefully divided angle scales, rods, chains, levels, and plumb bobs. The primary referent for elevations was mean sea level, already a problematic concept in view of changes of water level in response to tides, currents, and meteorological pressure changes. Individual countries established topographic surveys and used astronomical measurements to locate prime coordinate points. Nations with access to an ocean established elaborate gauging stations from which a time-average or *mean* sea level could be defined. Survey crews could carry this elevation reference inland by the use of levels and plumb bobs. Elevations of high and relatively inaccessible mountains were estimated barometrically, by comparing the pressure of the air at the top of the mountain to that at sea level. All of these methods, on close examination, amount to referring elevations to an equipotential surface. The equipotential that corresponds to mean sea level is called the geoid, and all elevations are, ideally, referred to this surface.

The geoid is quite hard to measure accurately. Although it roughly corresponds to a flattened sphere, as described previously, slight variations in density from one location to another gently warp it into a complex surface. Determination of the geoid thus requires precision measurements of the acceleration of gravity, as well as accurate leveling. Much of both classical and satellite geodesy is devoted to determining the geoid and, thus, permitting elevations to be defined with respect to a level surface (level in the sense of an equipotential, down which water will not run). Historically, each nation with a topographic survey created its own version of the geoid, although thanks to satellite measurements these are now knit into a consistent global network.

Elevations referred to the geoid are very convenient for a variety of purposes. Besides engineering applications, such as determining the true gradient of a canal or railway line, they are also essential to geologists who hope to estimate water discharges from the slope of a river system. The "upstream" ends of many river systems (the Mississippi is one) are actually closer to the center of the Earth than their mouths. And yet the water still flows from head to mouth because water flows from a higher to a lower gravitational potential.

The modern era of the Global Positioning System (GPS) is ushering in new changes. The orbiting GPS satellites really define positions with respect to the Earth's center of mass, so converting GPS elevations to elevations with respect to the geoid requires an elaborate model of the geoid itself. It has become common to refer elevations to a global average datum that locally may not correspond to the actual geoid.

The determination of elevations on other planets is becoming nearly as complex as that on Earth, thanks to a flood of new data from orbiting spacecraft. The first body to be orbited by a spacecraft capable of determining elevations precisely was the Moon. The Apollo orbiters carried laser altimeters that measured the elevations of features beneath their orbital tracks. Although it was many years before the Clementine spacecraft expanded

this method beyond the equatorial swaths cut by the Apollo orbiters, a prime reference surface for lunar elevations had to be chosen. Rather than trying to use the very slightly distorted equipotential surface, the reference surface was chosen to be a perfect sphere of radius 1738 km centered on the Moon's center of mass. All lunar topographic elevations are relative to this sphere. Since this sphere is not a geoid (although it is close enough for many purposes) care must be taken when, for example, estimating the slopes of long lava flows over the nearly level plains of the maria.

The topographic reference levels chosen for different planets varies depending on the rotation rate (and direction) of the planet, its degree of deviation from a sphere, and the technology available. The reference surfaces of Mercury and Venus are spheres. The mean diameter of Mercury has yet to be established: At the moment, the only global data set comes from radar measurements of equatorial tracks, but the MESSENGER laser altimeter should soon make a better system possible. The reference surface for Venusian elevations is a sphere of diameter 6051 km, close to the average determined by the Magellan orbiter.

Mars offers mapmakers serious problems when it comes to elevations. The Martian geoid is far from a rotationally symmetric spheroid, thanks to the large non-hydrostatic deviations caused by the Tharsis gravity anomaly. The geoid is intended to coincide with the level at which the mean atmospheric pressure equals 6.1 mb, the triple point of water. However, the atmospheric pressure varies seasonally by a substantial fraction of the entire pressure, so locating this point is not straightforward.

Some Martian elevation maps are referenced to a spheroid with flattening 1/170, a system recommended by the International Astronomical Union (IAU) (Seidelmann *et al.*, 2002). However, much of the high-precision data currently available is referenced to a more complex and realistic geoid, so that the user of such information must be alert to the system in use. Elevations with respect to a geoid are most useful in determining what directions are really downhill (that is, toward lower gravitational potential), which determines the expected flow direction of water or lava. Because geoids improve with time, no map of elevations is complete without a specification of the reference surface in use.

The surfaces of small asteroids such as Eros or Ida, comet nuclei such as Tempel 1, and many other small bodies that will be mapped in the future, present new problems. They are too irregular in shape to approximate spheres. At the moment their surface elevations are defined in terms of the distance from their centers of mass.

The gas giant planets in the outer Solar System lack solid surfaces and so elevations are especially difficult to define. The convention is now to refer elevations on these bodies to a spheroid at the 1-bar pressure level, which is a good approximation to an equipotential surface on such planets.

2.2.2 Elevation statistics: hypsometric curves

Elevation data can be processed and interpreted in many ways. A map of elevations, a topographic map, is certainly the most familiar and contains a wealth of data. However, one can extract more general features from such data that tell their own stories. On a small scale,

roughness is important for safely landing on and roving over planetary surfaces. Some of the methods for analyzing roughness are described in Box 2.1. On the large scale, an elevation plot known as the hypsometric curve has proven useful in highlighting general properties of planetary crusts.

A hypsometric curve is a plot of the percentage of the area of a planet's surface that falls within a range of elevations. Curves of this type have been constructed for the Earth ever since global topographic data sets became available and they show one of the Earth's major features. Figure 2.3c illustrates the Earth's hypsometric pattern, binned into elevation intervals of 500 m. The striking feature of this curve is the two major peaks in areas that lie between the maximum elevation of 7.83 km and the minimum of –10.376 km below mean sea level (note that these are not the highest and lowest points on the Earth – they are the highest and lowest elevations averaged over 5′ x 5′, 1/12-degree squares). A sharp peak that encompasses about 1/3 of the area of the Earth lies close to or above sea level. The second peak lies about 4 km below mean sea level and accounts for most of the rest of the Earth's area. These two peaks reflect the two kinds of crust that cover the surface of our planet. The low level is oceanic crust, which is thin (5–10 km), dense (about 3000 kg/m^3), basaltic in composition and young, being created by mid-oceanic spreading centers. The second principal topographic level is continental crust, which is much thicker (25–75 km) than oceanic crust, less dense (about 2700 kg/m^3), granitic in composition and much older than the ocean floors. Plate tectonics creates and maintains these two different crustal types.

Although Figure 2.3a shows a hypsometric curve for Mercury, the data set from which this is derived is sparse at the moment, consisting of a number of mostly equatorial radar tracks. At least with this data, however, there is no indication of an Earth-like dichotomy of crustal thickness.

Figure 2.3b illustrates the hypsometric curve of Venus, for which an excellent data set exists from the Magellan radar altimeter. This curve is an asymmetric Gaussian, skewed toward higher elevations. There is no indication of a double-peaked structure, from which we must infer that, whatever processes are acting to create the crust of Venus, they must differ profoundly from those that affect the Earth.

The Moon's hypsometric curve is illustrated in Figure 2.3d. Like Venus, the Moon lacks a dichotomy of crustal types, although there are important differences in elevation between the nearside and farside, illustrated by the thin lines that show separate hypsometric curves for the two hemispheres. This is generally attributed to systematic differences in crustal thickness between the nearside and farside, rather than compositional differences. The role of the large basins, especially the gigantic South Pole-Aitken basin, is still not fully understood.

Finally, we come to Mars in Figure 2.3e. Mars, surprisingly, shows a double-peaked distribution similar to that of the Earth. As shown by the light lines, the lower peak is accounted for by the Northern Lowlands, while the high peak represents the contribution of the Southern Highlands. The two terrains are divided by the Martian Crustal Dichotomy, an elliptical region tilted with respect to the north pole that may represent the scar of an

Box 2.1 **Topographic roughness**

The roughness of a surface is a concept that everyone is familiar with. Surprisingly, although there are many ways to measure roughness, there is no standard convention. Intuitively, rough surfaces are full of steep slopes, while smooth surfaces lack them. One measure of roughness would, thus, cite some statistical measure of the frequency of occurrence of a particular slope, extended over a range of slopes. For example, Root Mean Square (RMS) measures have often been used because they can be easily extracted from radar backscatter data. This statistic implicitly assumes that the distribution of slopes approximately follows a Gaussian curve, an assumption that needs to be tested. One might also cite mean or median slopes.

These simple statistical measures, while perhaps capturing our intuitive idea of *roughness*, do miss an important aspect of the concept, and that is the scale of the roughness. A surface that is smooth on a scale of 100 m might be very rough on the scale of 10 cm, a difference that is of overwhelming importance when one is trying to set a 1 m lander down safely onto a planetary surface. We thus need to define a baseline, L, in addition to the slope of a surface and to describe the statistics of slopes with respect to a range of baselines.

We could, for example, define the slope $s(L)$ of a surface for which we measure the elevations $z(x, y)$, where x and y are Cartesian coordinates that define a location on the surface. The surface slope is then given by:

$$s(L) = \frac{z(x,y) - z(x',y')}{L}. \tag{B2.1.1}$$

The points where the slope is evaluated, (x, y) and (x',y'), are separated by the distance $L = \sqrt{(x-x')^2 + (y-y')^2}$. On a two-dimensional surface we need some understanding of how to locate the different points at which elevations are evaluated, and many methods have been devised for this. At the present time, elevation data is often acquired by laser altimeters on orbiting spacecraft. The tracks along which elevations are measured are linear or gently curved, simplifying the decision process. New techniques may make this problem more acute, however: The laser altimeter aboard the Lunar Reconnaissance Orbiter now collects elevation data simultaneously from an array of five non-collinear spots, so that a full two-dimensional array of slopes can be defined.

A promising statistic is derived from fractal theory, the Hurst exponent, and has been applied to the analysis of Martian slopes in the MOLA dataset (Aharonson and Schorghofer, 2006). This statistic, at present, is limited to linear sets of elevation data, $z(x)$, in which the y coordinate is ignored. The variance $v(L)$ of the elevation differences along the track is computed for a large number N of equally-spaced locations:

$$v(L) = \sqrt{\frac{1}{N}\sum_{i=1}^{N}\left[z(x_i) - z(x_i + L)\right]^2}. \tag{B2.1.2}$$

The roughness is thus given by the slope $s(L)$:

$$s(L) = \frac{v(L)}{L} = s_0\left(\frac{L}{L_0}\right)^{H-1}. \tag{B2.1.3}$$

Box 2.1 **(cont.)**

It is often found that the variance $v(L)$ is a power function of the baseline L, so that if the variance is compared to the slope s_0 at some particular baseline L_0, a relation expressed by the second term in (B2.1.3) is found with an exponent H known at the *Hurst exponent*. Whether this exponent is constant over a broad range of baselines or depends in some simple way upon the scale is not yet known, nor is it understood how surface processes are related to this exponent, although some proposals have been made (Dodds and Rothman, 2000). More progress can be expected as more closely spaced elevation data is collected on a number of different planets.

A disadvantage of the definition (B2.1.2) is that a long, smooth slope also contributes to the variance because the elevations $z(x)$ on a straight slope differ by a constant amount along the track. One would really like to filter out all elevation differences except those close to the scale L. One solution to this problem is the median differential slope, which is based upon four points along the track. The two extreme points are used to define a regional slope, which is then subtracted from the elevation difference of the two inner points to achieve a measure of slope that is not affected by long straight slopes, but responds to short wavelength variations on the scale of the distance between the inner points (Kreslavsky and Head, 2000). The array of four points is located at $-L$, $-L/2$, $L/2$, and L around an arbitrary zero point that slides along the spacecraft track. This differential slope s_d is given by:

$$s_d(L) = \frac{z(L/2) - z(-L/2)}{L} - \frac{z(L) - z(-L)}{2L}. \qquad \text{(B2.1.4)}$$

The first term is the slope between the inner points and the second term is the larger scale slope. The differential slope is zero for a long straight slope, as desired.

In the past, the study of roughness tended to focus on landing-site safety, but current efforts are also making progress on extracting information on the surface processes creating the roughness. One may expect to hear more about this in the future.

ancient giant impact. Do these two peaks represent two types of crust, as on the Earth, or are these just areas with very different crustal thickness? We do not believe that Mars possesses plate tectonics, although it has been suggested that some plate processes may have acted in the distant past.

The Martian hypsometric curve offers an interesting lesson in the importance of referencing elevations to the geoid. Earlier plots of Mars elevations showed a Gaussian-like distribution of elevations similar to that of Venus or the Moon. Only after a good gravity field was measured and elevations referenced to a true geoid did the double-peaked character of Martian elevations become apparent.

2.2.3 Where are we? Latitude and longitude on the planets

Latitudes and longitudes are the conventional means for locating features on the surface of a planet. However, before such a system can be defined, the pole of rotation must be established. All systems of latitude and longitude are oriented around the north pole, which must

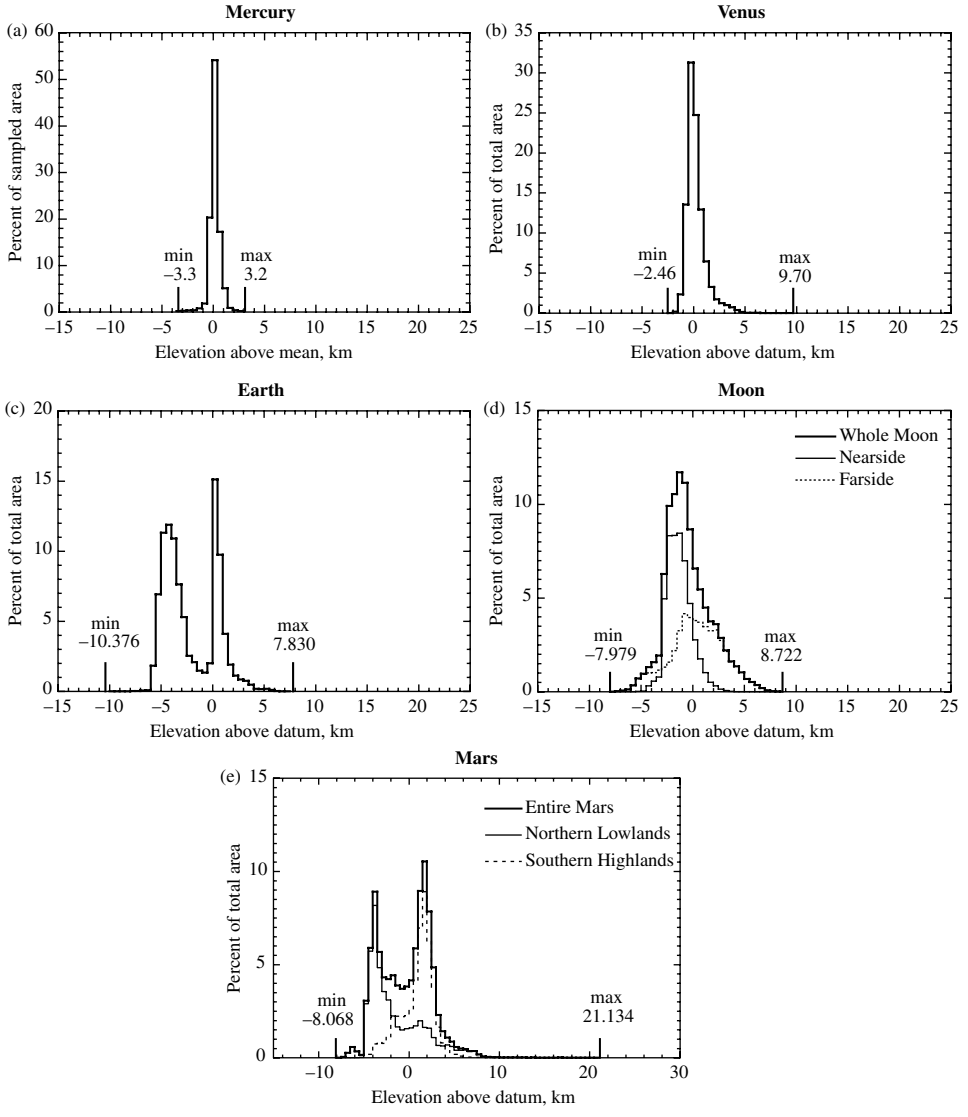

Figure 2.3 Hypsometric curves of the terrestrial planets and the Moon. Maximum and minimum elevations are also shown. These elevations refer to the maximum and minimum elevations averaged over square sample areas of different sizes, not the highest and lowest points on the planet's surface. (a) Mercury data from 9830 radar elevations in PDS file allMerc.txt. (b) Venus hypsometric curve derived from a 1° x 1° Magellan map of Venus from PDS dataset MGN-V-RDRS-5-TOPO-L2-V1.0, file TOPOGRD-DAT. (c) Earth, data is binned in 1/12 degree squares, from National Geophysical Data Center file TBASE.BIN. (d) Moon, data is ¼ degree data from Clementine LIDAR from PDS dataset CLEM1-L-LIDAR-5-TOPO-V1.0, file TOPOGRD2.DAT. Light lines show separate curves for the nearside and farside. (e) Mars, ¼ degree MOLA gridded data from PDS dataset MGS-M-MOLA-5-MEGDR-L3-V1.0, file MEGT90N000CB.IMG. Light lines show data separately for the Northern and Southern crustal provinces. For this purpose, the planet was divided into two hemispheres by a great circle whose pole is located at 53° N and 210° E longitude.

be determined in some absolute system of coordinates. The locations of the Earth's poles are determined astronomically, by the position of the extrapolated rotation axis among the stars in the sky. Although the Earth's axis precesses slowly with a period of about 26 000 yr, this gradual change is predictable and can be taken into account when referring to the pole position by citing the time, or epoch, at which the position is cited. The pole positions of the other planets are defined in a similar way, in terms of the celestial coordinates, the declination and right ascension, of their projected northern axis of rotation.

The choice of prime meridian for different planets is entirely arbitrary, but must be a definite location. On the Earth, we use the longitude of a point in Greenwich, UK, as the zero of longitude. On Mercury a crater known as Hun Kal defines the location of the 20° longitude. The choice of the 0° longitude on Venus fell to the central peak of a crater known as Ariadne, while on Mars the 0° longitude passes through a small crater known as Airy-0. Pluto's 0° of longitude (at present) passes through the mean sub-Charon point. As new bodies are mapped and their rotation axes determined, new choices for the prime meridian have to be made.

The prime meridians of the fluid gas giant planets in the outer Solar System are much harder to define and are based on the rotation rates of their magnetic fields rather than the shifting patterns of clouds in their atmospheres. Because the clouds rotate at different rates depending on latitude, they do not yield definite rotation rates for the entire planet. For these planets an accurate rotation rate must be determined and that rotation rate, plus the epoch at which it was established, defines the prime meridian.

Venus presents an interesting cartographic problem because its spin is retrograde. Its north pole, nevertheless, lies on the north side of the ecliptic by convention and, also by cartographic convention, longitudes increase eastward from 0° to 360°.

The International Astronomical Union adopted a convention in 2000 that defines the latitude and longitude coordinate system used in locating features on the surface of planets. The first principle defines the north pole of a Solar System body:

(1) The rotational pole of a planet or satellite that lies on the north side of the invariable plane will be called north, and northern latitudes will be designated as positive.

The second principle is more controversial and there is some disagreement between geophysicists and cartographers about the most sensible way to present longitudes:

(2) The planetographic longitude of the central meridian, as observed from a direction fixed with respect to an inertial system, will increase with time. The range of longitudes shall extend from 0° to 360°.

Thus, west longitudes (i.e., longitudes measured positively to the west) will be used when the rotation is prograde and east longitudes (i.e., longitudes measured positively to the east) when the rotation is retrograde. The origin is the center of mass. Also, because of tradition, the Earth, Sun, and Moon do not conform with this definition. Their rotations are prograde and longitudes run both east and west 180°, or east 360° (Seidelmann *et al.*, 2002).

This convention means that Mars presents a left-handed coordinate system, a consequence not favored by geophysicists. This debate is not resolved at the present time, so the user of cartographic data must carefully check what conventions are in use – it is very easy to download geophysical data for Mars and find that one is working on a mirror image of the actual planet Mars.

2.3 Spectral representation of topography

Maps showing contours of elevation are not the only way of codifying topographic information. Just as any function of spatial coordinates can be broken down into a Fourier series in an inverse space of wavenumbers, topography can be represented as a sum of oscillating functions on a sphere. This mode of representation is known as harmonic analysis or spectral analysis and for many data sets is preferred over a purely spatial representation.

Spectral analysis averages elevations over all positions on a sphere and presents the information as a function of wavelength, not position. No information is lost in this process: With the appropriate mathematical tools one can freely transform from space to wavelength and back again.

The full details of harmonic analysis are too specialized for full presentation in this book. The interested reader is referred to a fine review of the entire subject by Wieczorek (2007). In this book it is enough to note that any function of latitude φ and longitude λ, such as elevation $H(\varphi,\lambda)$, can be expressed as:

$$H(\varphi,\lambda)=\sum_{l=0}^{\infty}\sum_{m=-l}^{l}H_{lm}Y_{lm}(\varphi,\lambda) \tag{2.10}$$

where l and m are integers and the $Y_{lm}(\varphi,\lambda)$ are spherical harmonic functions of order l and degree m. They are given in terms of more standard functions as:

$$Y_{lm}(\varphi,\lambda)=\begin{cases}\bar{P}_{lm}(\sin\varphi)\cos m\lambda & \text{if } m\geq 0\\ \bar{P}_{l|m|}(\sin\varphi)\sin|m|\lambda & \text{if } m<0\end{cases} \tag{2.11}$$

where the $\bar{P}_{lm}$ are normalized associated Legendre functions given by:

$$\bar{P}_{lm}(\sin\varphi)=\sqrt{(2-\delta_{0m})(2l+1)\frac{(l-m)!}{(l+m)!}}P_{lm}(\sin\varphi) \tag{2.12}$$

where δ_{ij} is the Kronecker delta function and P_{lm} are the standard, unnormalized Legendre functions. These functions are tabulated in standard sources and, more importantly, can be computed with readily available software. There are many issues about the conventional normalizations of these functions, which are not standardized across all scientific disciplines.

The functions Y_{lm} are the spherical analogs of sines and cosines for Fourier analysis. They are simple for small-order l and become more complex, with more zero crossings, as l increases. They possess $2|m|$ zero-crossings in the longitudinal direction and $l - |m|$ in the latitudinal direction. Thus Y_{00} is a constant, Y_{10}, Y_{1-1}, and Y_{11} correspond to the displacement of a sphere from the center of mass (for example, a center-of-figure, center-of-mass offset) and the five $l = 2$ terms describe an oblate or triaxial tidally distorted sphere. In general, as l increases the wavelength of the feature that can be represented by these harmonics decreases. This is made more precise by an approximate relation between the wavelength w of features that can be represented by spherical harmonics of order l: $w \approx 2\pi a / \sqrt{l(l+1)}$, where a is the planetary radius.

The expansion of topography in spherical harmonics makes the idea of orders of relief precise: The zeroth-order harmonic is just the radius, the first is the center-of-mass center-of-figure offset, the second is the rotational or tidal distortion, etc. Harmonic coefficients for the topography of the planets to degree and order 180 are becoming common, and still higher degrees exist for the Earth and are planned for the other planets as sufficiently precise data becomes available. In addition to topography, the geoid and gravity fields are also represented by spherical harmonics, a format that makes many computations of, for example, global isostatic compensation, much simpler than it is for spatial data.

The spherical harmonic functions are orthogonal after integration over the complete sphere, so that the harmonic coefficients H_{lm} can be obtained from the topography $H(\varphi,\lambda)$ by:

$$H_{lm} = \frac{1}{4\pi} \int_0^{2\pi} \int_{-\pi/2}^{\pi/2} H(\varphi,\lambda)\, Y_{lm}(\varphi,\lambda) \cos\varphi \, d\varphi \, d\lambda. \tag{2.13}$$

One can freely pass from the spatial representation of topography to the harmonic representation and back again. There is no loss of information, nor any saving in the amount of data to be stored for one or the other representation.

Just as the hypsometric function attempts to distil useful global information from the map of elevations, a similar extraction of data is often made from the harmonic coefficients. This data contraction is called the spectral power and is a measure of how much of the topography is due to a particular wavelength. The RMS spectral power density collapses a full set of l^2+2l+1 numbers for harmonic coefficients to degree and order l down to a set of only l numbers by summing over all orders for each degree:

$$S_l = \sqrt{\sum_{m=-l}^{l} H_{lm}^2}\,. \tag{2.14}$$

The RMS spectral power densities given by Equation (2.14) are plotted in Figure 2.4 for each of the terrestrial planets (excluding Mercury) and the Moon. Except for the Moon, most of the RMS power densities on this plot rise with increasing wavelength, so each body

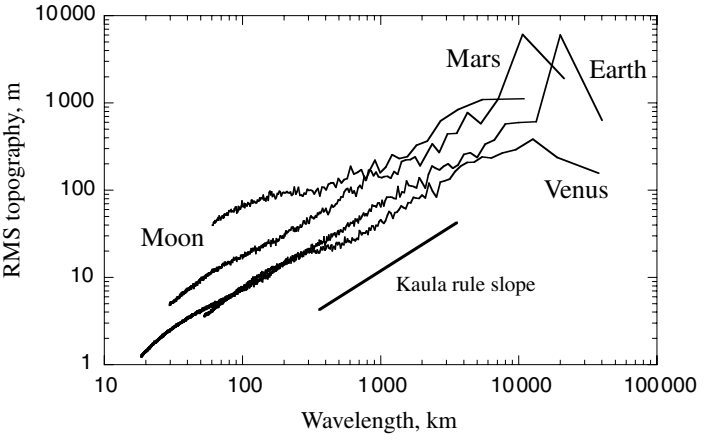

Figure 2.4 Topographic power spectra of the terrestrial planets and the Moon, excluding Mercury for which the necessary data does not yet exist. Lunar spectral data are from the Kaguya data set (Araki *et al.* 2009). Spectral data on Earth, Venus, and Mars are from Mark Wieczorek's website, http://www.ipgp.fr/~wieczor/SH/SH.html, files SRTMP2160, VenusTopo719.shape and MarsTopo719.shape, respectively.

has more power in longer-wavelength topography. Another way of saying this is that the slopes of the surfaces are approximately independent of their scale. It is popular to call this a fractal relationship, but it is unclear, at present, exactly what this means. The Earth and Venus are comparably smooth at short wavelengths, while Mars is rougher than both and the Moon is rougher still. The Moon's roughness does not rise with increasing wavelength as fast as that of the larger planets.

William Kaula worked extensively on harmonic representations of topography and his studies of the Earth's topography led him to formulate what we will call here "Kaula's second law," which is that the RMS topography depends on the inverse order, $1/l$. Because wavelength depends on the inverse order as well, his law states that the power is directly proportional to the wavelength. The prediction of this law is shown on Figure 2.4 and it does seem to hold fairly well for the major planets, but not for the Moon. The deviation shown here for the Moon is relatively new: It was not known before the data from the Kaguya laser altimeter were analyzed.

Spectral representations are, at present, difficult to interpret (see, e.g. the discussion by Pike and Rozema, 1975). Spectral data at a very small scale is widely used for computations of "trafficability" of vehicles across terrains and for designing vehicle suspension systems, but its use in geologic interpretation has been limited. The reason for this may be that the spectral method averages over a wide variety of different terrain types that are shaped by different processes and so loses the signatures characteristic of individual processes. Whatever the reason, it is currently an analysis technique in search of an interpretation, although some suggestive models have provided more insight into the interpretation of such data (Dodds and Rothman, 2000).

Further reading

Newton's Principia is tough going, but full of surprising results. It is astonishing how far Newton went with the theory of the Earth's figure (Newton, 1966). You do not need to know Latin to read the translation of the Principia, but you do need to be patient and resourceful. Harold Jeffreys was deeply interested in the figure of the Earth, the Radau approximation, and the theory of the Moon's triaxial figure. There are six editions of his famous book *The Earth*, but the third (Jeffreys, 1952) and fourth present the apex of his insight into this problem. The problem of determining the shape of the Earth has been of major interest to astronomers and mathematicians since Newton. The early history of investigation of the figure of the Earth is exhaustively told in the full language of mathematics by Todhunter (1962). More modern extensions are well covered in Chandrasekhar (1969) and Jardetzky (1958). Kaula's book (Kaula, 1968) is now very dated in its facts, but he covered many of the methods of planetary geophysics, particularly geodesy, in great detail. The nature of the geoid on Earth and its determination are well discussed in Lambeck (1988). The details of modern planetary cartography are described in book form by Greeley and Batson (2000). Spectral analysis of both topography and gravity are the subjects of a very recent and very clear review by Mark Wieczorek (2007) that offers the simplest introduction to spherical harmonics that I am aware of. He also goes to some trouble to explain the different normalization conventions in the geophysical literature.

Exercises

2.1 A whirling moon

Saturn's moon Iapetus is currently synchronously locked to Saturn, with a rotation (and orbital) period of 79.3 days. In spite of its slow rotation, Iapetus has a considerable equatorial bulge, a–c ≈ 35 km (Table 2.3). Iapetus' density is not very different from that of water ice, so it can be treated as an approximately homogeneous body. If Iapetus' equatorial bulge is a fossil remnant from a time when it was spinning faster than at present, estimate the minimum initial period of Iapetus' rotation (explain why this is a minimum estimate). What do you think may have happened to Iapetus?

2.2 Hot Jupiteus shaped like water melons

Planet WASP-12b circles a Sun-like star about 600 light years from Earth in the constellation Auriga. It is a *hot Jupiter* planet, with a mass equal to 1.41 times that of Jupiter, radius 1.83 times larger than Jupiter, but circles only 0.0229 AU (Astronomical Units) from its star with a period of 1.0914 days. Use Equations (2.6) and (2.7), suitably generalized for a planet orbiting a star, to compute the tidal distortion of this planet, assuming that it is synchronously locked to its star (which is almost certainly true). Tabulate the lengths of the three principal axes a, b, and c. What do you think this implies for the planet? For more on this system, see Li *et al.* (2010).

2.3 The axis of least effort

The kinetic energy of rotation of a body with a principal moment of inertia I about some axis is given by $E = \frac{1}{2} I\omega^2$, where ω is the angular rotation rate (radians/s). The angular momentum L of a rotating body is given by $L = I\omega$. For fixed angular momentum, show that the kinetic energy of a rotating body is a minimum if it rotates about the axis with the maximum moment of inertia C of the three principal moments $C \geq B \geq A$.

Extra Credit: If a body is rotating stably about its C axis and some internal process in the body redistributes its internal mass and switches the C and B principal axes, what happens to this body? Note that a process of this kind has been proposed for, among others, Enceladus (Nimmo and Pappalardo, 2006).